Gravitational collapse of massless scalar field and cosmic censorship

Dalia S. Goldwirth
The Racah Institute for Physics, The Hebrew University, Jerusalem, Israel

Tsvi Piran
The Racah Institute for Physics, The Hebrew University, Jerusalem, Israel, and The Institute for Advanced Study, School of Natural Sciences, Princeton, New Jersey 08540
(Received 24 February 1987)

We present a numerical study of the gravitational collapse of a massless scalar field. We calculate the future evolution of new initial data, suggested by Christodoulou, and we show that in spite of the original expectations these data lead only to singularities engulfed by an event horizon.

I. INTRODUCTION

Christodoulou[1-5] has recently shown that for a sufficiently weak, initial spherical massless scalar field there exists a regular solution for an arbitrary long time for the coupled general-relativistic and scalar field equations. This result is the first proof of existence of long-time solutions to Einstein equations. He has shown that the scalar field converges toward the origin, bounces, and disperses to infinity. One expects a gravitational collapse to a black hole when the initial field is stronger. However, it has not been shown, yet, that a black hole rather than a naked singularity forms. The conjecture that a black hole forms is a special case of the cosmic censorship hypothesis.[6] We have studied, numerically, the collapse of a massless scalar field using a characteristic method.[7] We find that while weak fields bounce and disperse to infinity, strong initial fields collapse into a black hole. A similar behavior was observed by Choptuik[8] who solved, independently, the same problem using the $3+1$ formalism and finite-differencing numerical techniques. Our discussion is focused on the evolution of special initial data which were suggested by Christodoulou[9] as possibly leading to a naked singularity. We show that it is unlikely that these initial data will produce a naked singularity. Recently, Christodoulou has observed[10] that this initial data represent a generic approach towards a singularity of a collapsing massless scalar field. This observation combined with our results is a step toward the proof of cosmic censorship.

II. THE EVOLUTION EQUATIONS

We express the metric of a spherically symmetric spacetime in the form

$$ds^2=-g\bar{g}\,du^2-2\frac{g}{\bar{g}}du\,dr+r^2d\Omega^2\ . \tag{2.1}$$

We define, following Christodoulou,[1-5]

$$\phi=\bar{h}=\frac{1}{r}\int_0^r h\,dr\ . \tag{2.2}$$

The nonvanishing components of the energy-momentum tensor of the massless scalar field are $T_{rr}=\bar{h}_{,r}{}^2$ and $T_{ru}=T_{ur}=\frac{1}{2}\bar{g}\bar{h}_{,r}{}^2$, and the nontrivial Einstein equations are

$$G_{rr}=\frac{2}{r}\frac{g_{,r}}{g}=8\pi\bar{h}_{,r}{}^2 \tag{2.3}$$

and

$$G_{ru}=\frac{2}{r^2}\bar{g}\left[\frac{g}{\bar{g}}+r\left[\frac{g_{,r}}{g}-\frac{\bar{g}_{,r}}{g}\right]-1\right]=8\pi\bar{g}\bar{h}_{,r}{}^2\ . \tag{2.4}$$

Regularity at the origin requires $g(u,0)=\bar{g}(u,0)$. The boundary condition $h(u,0)=\bar{h}(u,0)$ forces us to integrate the equations outward and to impose the normalization $g(u,0)=\bar{g}(u,0)=1$ (which corresponds to selecting the time coordinates as the proper time of an observer at the origin), rather than the common $g(u,\infty)=\bar{g}(u,\infty)=1$. With these conditions the solution at r depends only on the solution at $r'<r$ and we can integrate Eqs. (2.3) and (2.4):

$$g=\exp\left[4\pi\int_0^r\frac{(h-\bar{h})^2}{r}dr\right] \tag{2.5}$$

and

$$\bar{g}=\frac{1}{r}\int_0^r g\,dr\ . \tag{2.6}$$

The incoming light geodesics, satisfying the ordinary differential equation $dr/du=-\frac{1}{2}\bar{g}(u,r)$ are the characteristics of the problem. Using the characteristic method we convert the scalar field evolution equation

$$h_{,u}-\tfrac{1}{2}\bar{g}h_{,r}=\tfrac{1}{2}(g-\bar{g})(h-\bar{h}) \tag{2.7}$$

into a pair of coupled differential equations

$$\frac{dh}{du}=\frac{1}{2r}(g-\bar{g})(h-\bar{h}) \tag{2.8a}$$

and

$$\frac{dr}{du}=-\tfrac{1}{2}\bar{g}\ , \tag{2.8b}$$

TABLE I. Formation of a black hole with Gaussian initial data.

A	$\max(2M/r)$	$u_{\rm bh}$	$r_{\rm bh}$
1.874 5	0.98	0.633 6	0.008 99
1.89	0.986	0.576	0.030 26
2.05	0.992	0.482 4	0.065 3
2.3	0.992	0.396	0.098 8
2.5	0.992	0.345 6	0.121 6

which we solve together with the integral equations (2.5) and (2.6).

The mass contained within the sphere of radius r (at a retarded time u), $M(u,r)$, equals

$$M(u,r)\equiv\frac{r}{2}\left[1-\frac{\bar{g}}{g}\right] . \tag{2.9}$$

Using

$$\frac{\partial M}{\partial r}=2\pi\frac{\bar{g}}{g}(h-\bar{h})^2$$

we express M as

$$M=2\pi\int_0^r\frac{\bar{g}}{g}(h-\bar{h})^2dr . \tag{2.10}$$

$2M/r$ provides a measure on the strength of the gravitational field. A black hole forms when $2M/r_h=1$. $2M/r_h=1$ requires that $\bar{g}/g=0$. With the normalization $g(\infty)=1$, g and $\bar{g}$ are finite everywhere. The horizon cannot be crossed, but g and $\bar{g}$ approach zero as the interior approaches a black hole.[11] With the normalization $g(u,0)=\bar{g}(u,0)=1$, g diverges on r_h and $\bar{g}$ diverges as we approach the same outgoing null geodesic. The divergence of the metric function forces us to stop the evolution before the horizon forms. However, we can infer on black-hole formation from the divergence of the metric functions and from the fact that $2M/r\to 1$. In fact, we can reach $2M/r$ values as high as 0.99 (see Table I).

III. THE NUMERICAL SOLUTION

To solve numerically Eqs. (2.8a) and (2.8b) we define a radial grid r_n, where $n=1,\ldots,N$. Each grid point represents a radial null geodesic. Equations (2.8a) and (2.8b) become a set of $2N$ coupled differential equations

$$\frac{dh_n}{du}=\frac{1}{2r_n}(g_n-\bar{g}_n)(h_n-\bar{h}_n) , \tag{3.1a}$$

$$\frac{dr_n}{du}=-\tfrac{1}{2}\bar{g}_n , \tag{3.1b}$$

where h and g satisfy the boundary conditions

$$\bar{h}_1=h_1,\quad g_1=\bar{g}_1=1 . \tag{3.2}$$

Equations (3.1a) and (3.1b) include implicitly integration along r, for a fixed u, to obtain $\bar{h}$, g, and $\bar{g}$. We write these integrals as

$$\bar{h}_n=\frac{1}{r_n}\sum_{i=1}^{n}\omega_i h_i , \tag{3.3a}$$

$$g_n=\exp\left[4\pi\sum_{i=1}^{n}\omega_i\frac{(h_i-\bar{h}_i)^2}{r_i}\right] , \tag{3.3b}$$

$$\bar{g}_n=\frac{1}{r_n}\sum_{i=1}^{n}\omega_i g_i , \tag{3.3c}$$

where the coefficients ω_i are determined by a three-point Simpson method for unequally spaced abscissas. (Even if the grid is evenly spaced initially, it will not remain so during the evolution, see Fig. 1.) The integration is based on overlapping parabolas. We solve the equation

$$f(r)\simeq a_n r^2+b_n r+c_n \tag{3.4a}$$

for r_{n-2}, r_{n-1}, and r_n to obtain a_n, b_n, and c_n and then we evaluate the integral I_n at r_n as

$$\begin{aligned}I_n&=I_{n-2}+\int_{r_{n-2}}^{r_n}f(r)dr\\&=I_{n-2}+\frac{a_{n-2}+a_n}{2}\left[\frac{r_n{}^3-r_{n-2}{}^3}{3}\right]\\&\quad+\frac{b_{n-2}+b_n}{2}\left[\frac{r_n{}^2-r_{n-2}{}^2}{2}\right]\\&\quad+\frac{c_{n-2}+c_n}{2}(r_n-r_{n-2}) .\end{aligned} \tag{3.4b}$$

Specifically,

$$\bar{h}_n=\frac{1}{r_n}\left[\bar{h}_{n-2}r_{n-2}+\sum_{i=n-2}^{n}\omega_i h_i\right] , \tag{3.5a}$$

$$g_n=\exp\left[\ln g_{n-2}+4\pi\sum_{i=n-2}^{n}\omega_i\frac{(h_i-\bar{h}_i)^2}{r_i}\right] , \tag{3.5b}$$

$$\bar{g}_n=\frac{1}{r_n}\left[\bar{g}_{n-2}r_{n-2}+\sum_{i=n-2}^{n}\omega_i g_i\right] . \tag{3.5c}$$

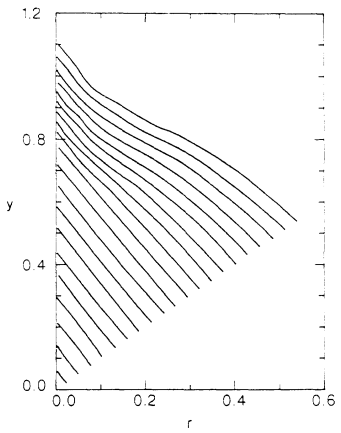

FIG. 1. Null geodesics (for $A=1.8$) in the r and $y=r+\sqrt{2}u$ plane. Note the convergence along the evolution.

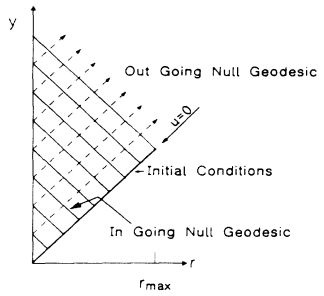

FIG. 2. Null trajectory in the r and $y=r+\sqrt{2}u$ plane. The scalar field bounces from the origin and disperses "instantaneously" to infinity, along the outgoing null geodesic $u=$const.

For $n=2$ we use the trapezium rule

$$I_2=\tfrac{1}{2}[f(r_1)+f(r_2)](r_2-r_1)\ . \tag{3.6}$$

We solve the $2N$ ordinary differential equations using three different standard methods: the sixth-order Runge-Kutta, twelfth-order implicit Adams, and fifth-order Gear's methods.[12]

The time step du is determined so that in each step the change in the null trajectory r_n is less half the distance between it and the null trajectory r_{n-1}: i.e.,

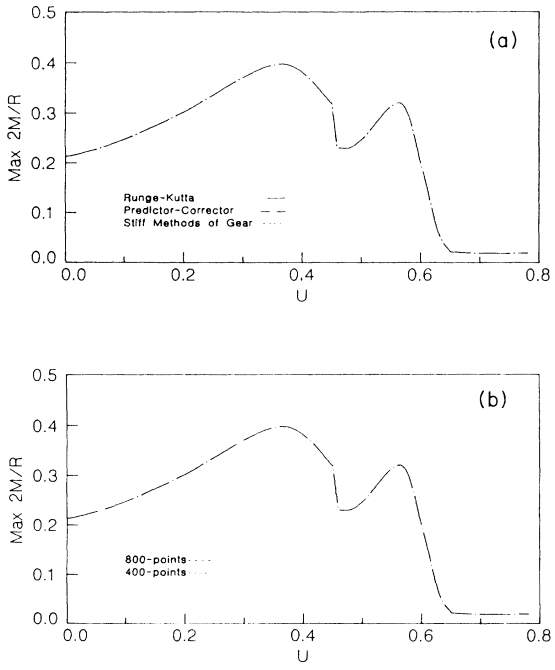

FIG. 3. max$(2M/r)$, using $A=1.8$, vs u: (a) Comparison between three different numerical methods for solving ordinary differential equations; (b) comparison between two different grid sizes along r. The numerical errors are so small that the different lines in (a) and (b) overlap.

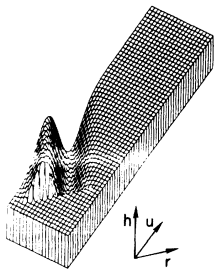

FIG. 4. h in the Newtonian case is constant along the null geodesics (vertical scale of 0–0.0012).

$$du<\frac{r_n-r_{n-1}}{\bar{g}_n}\ . \tag{3.7}$$

Once a null trajectory arrives at the origin $r=0$, it bounces and disperses "instantaneously" along the outgoing null geodesic $u=$const to infinity (see Fig. 2). At this stage we exclude this grid point from the solution. The calculation comes to its end when all the matter arrives at the origin and disperses to infinity, i.e., when $r_N=0$. When the initial field is weak, $\bar{g}_n\simeq 1$ and the calculation ends at the retarded time $u_{\text{final}}\simeq 2r_N$. u_{final} decreases when the initial field increases.

As we approach the stage when a black hole forms $\bar{g}_n\to\infty$, condition (3.7) yields $du\to 0$ and stops the calculation before the horizon appears. $r_N=0$ is not reached. We identify the horizon's location from the maximal value of $2M/r$. A typical value is 0.99 (see Table I).

When we ignore the gravitational field ($g=\bar{g}=1$), the solution is trivial:

$$h(u,r_n(u))=h(0,r_n)\ , \tag{3.8a}$$

$$r_n(u)=r_n(0)-\tfrac{1}{2}u\ . \tag{3.8b}$$

We use this solution to check the computer code. Although it is a weak check since the differential equations are trivial in this case, it still provides a basic check on the logic of the code. Moreover, a solution of the relativistic equations (3.1a) and (3.1b) satisfies approximately Eqs. (3.8a) and (3.8b) when the gravitational effects are negligible.

We use the errors in max$(2M/r)$ as a measure for the combined accumulated numerical errors. Using $A=1.8$

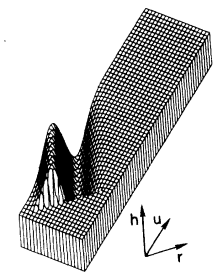

FIG. 5. h for a very weak gravitational field $A=0.01$. The solution is similar to the Newtonian case.

TABLE II. The range of the maximal values of various functions, comparison between the Newtonian case and the weak-gravitational-field case.

Functions	Newtonian case	$A=0.01$
h	$0.121\,221\,6\times10^{-2}$	$(0.121\,221\,6-0.121\,221\,7)\times10^{-2}$
$\bar{h}$	$(0.490\,8-1.212\,216)\times10^{-3}$	$(0.490\,8-1.212\,216)\times10^{-3}$
g	1	1.000 010–1.000 017
$\bar{g}$	1	1.000 005–1.000 012
$2M/r$	$(0.053-0.087)\times10^{-5}$	$(0.67-1.094)\times10^{-5}$

(see next section), for which the gravitation field is already quite strong, we have checked the integration along r by comparing calculations with two grids with 400 and 800 points. The largest absolute error (which appeared toward the end of the calculation), was less than 10^{-4} [Fig. 3(a)]. The largest relative error was 3%. We have checked the integration along u by comparing three different integration methods. Comparison of the solutions revealed differences of about 10^{-6} [Fig. 3(b)].

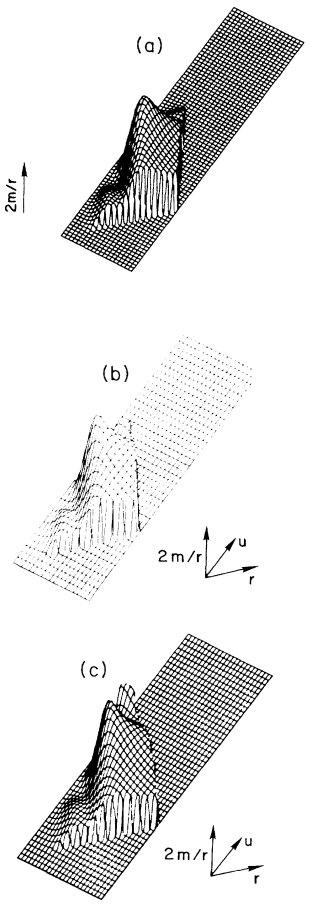

FIG. 6. $2M/r$ for various initial conditions. (a) $A=0.01$, a very weak gravitational field (vertical scale of $0-1.094\times10^{-5}$). (b) $A=1.5$, the gravitation field is of moderate strength (vertical scale of 0–0.25). (c) $A=1.8$, strong gravitation field (vertical scale of 0–0.37).

IV. NUMERICAL RESULTS

We have chosen an initial Gaussian ϕ:

$$\phi(u=0,r)=\bar{h}(u=0,r)$$
$$=Ar^2\exp\left[-\left[\frac{r-x_0}{D}\right]^2\right] \tag{4.1}$$

with $D=0.1$, $x_0=0.2$, and $r_N=0.54$ on a grid of 400 points in the radial direction. The Newtonian solution is shown in Fig. 4. It can be seen (Table II) that the numerical results agree with the analytic solution (3.8a) and (3.8b).

We have performed a series of relativistic calculations for different values of A. For a small amplitude, e.g., $A=0.01$, the gravitational effects are negligible and the results are similar to the Newtonian ones (see Table II and Fig. 5). Comparison of $2M/r$ for $A=0.01$ with the Newtonian results, shows that it is slightly larger, which is not surprising since g and $\bar{g}$ are not exactly 1.

The change of the maximum value of $2M/r$ achieved along the evolution, as a function of A, is shown in Table III. For $A<0.1$ the gravitation field is very weak and the scalar field simply bounces and disperses to infinity. An increase of the strength of the initial field leads to an increase in $2M/r$ and causes the null geodesics to converge. A second peak appears in $2M/r$ when the amplitude of A increases (see Fig. 6). A black hole appears when $A\geq1.8745$ (see Fig. 7). In fact, our calculation stops, due to the divergence of the metric

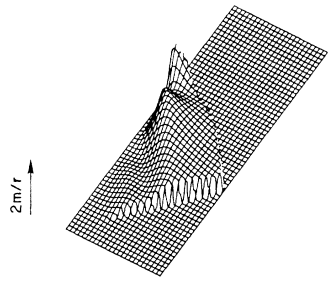

FIG. 7. $2M/r$ for $A=1.8745$ (vertical scale of 0–1). The formation of a black hole can be seen when $2M/r$ approaches unity.

TABLE III. The range of $\max(2M/r)$ for various initial scalar fields.

A	$\max(2M/r)$	u_f
0.01	$(0.67-1.094)\times10^{-5}$	1.08
0.1	$(0.67-1.093)\times10^{-3}$	1.08
1.1	0.077 42–0.109 3	1.036 8
1.5	0.138–0.249 6	0.943 2
1.8	0.191 5–0.372 8	0.799 2
1.85	0.200 83–0.399 7	0.741 6

functions, just before the apparent horizon forms (see Table I). As A increases, a black hole forms earlier and with a larger final mass M_f. The graph of M_f/M_i (M_i being the initial mass) as function of A, displays a jump at $A=1.8745$: below that value $M_f=0$, above it M_f has a finite value (see Fig. 8).

V. CHRISTODOULOU'S SPECIAL SOLUTION

We address now the question of whether or not it is possible to choose initial data which will evolve into a naked singularity. In an unpublished work, Christodoulou[9] has suggested that one consider, as initial data at $u=-1$, a scalar field whose future evolution satisfies

$$\phi(u,r)\equiv\bar{h}(u,r)=\bar{h}(-1,r/|u|)-\kappa\ln(|u|)\ . \tag{5.1}$$

We define

$$\bar{h}(-1,x)=-\int_x^\infty\theta(\bar{x})d\bar{x}\ , \tag{5.2}$$

where $x=r/u$ leads to

$$h(u,r)=h(-1,r/|u|)-\kappa\ln(|u|)-x\theta(x)\ , \tag{5.3a}$$

$$g(u,r)=\exp\left[4\pi\int_0^{x|u|}|u|x\theta^2(x)dx\right]$$

$$=g(-1,r/|u|)\ , \tag{5.3b}$$

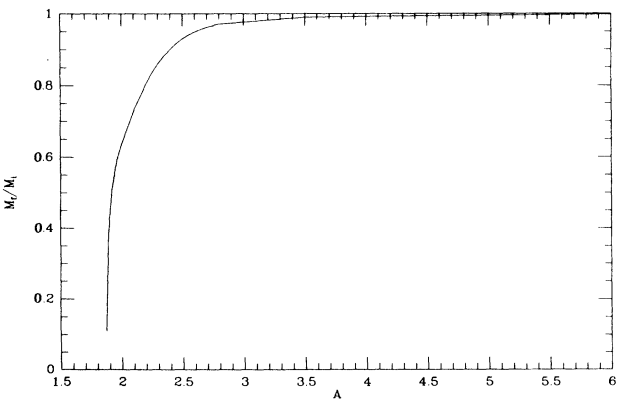

FIG. 8. M_f/M_i vs A for $A\geq1.8745$.

and

$$\bar{g}(u,r)=\frac{1}{r}\int_0^{r/|u|}g(-1,r/|u|)|u|d(r/|u|)$$

$$=\bar{g}(-1,r/|u|)\ . \tag{5.3c}$$

The requirement that ϕ satisfies the evolution equation (2.7) yields an ordinary differential equation for θ:

$$x(\tfrac{1}{2}\bar{g}-x)\frac{d\theta}{dx}=\kappa-\theta(x)[\tfrac{1}{2}(g+\bar{g})-2x]\ . \tag{5.4}$$

Equation (5.4) together with Eqs. (5.3b) and (5.3c), specify the initial data for $0\leq r\leq x_1$. The left-hand side of Eq. (5.4) vanishes at x_1, where $x_1=\frac{1}{2}\bar{g}$ and a solution satisfying Eq. (5.1) does not exist for $r>x_1$. With the initial data for ϕ given at $u=-1$, ϕ becomes singular at $r=0$, $u=0$ and is regular elsewhere for $-1\leq u\leq0$. Therefore, it is a potential counterexample to cosmic censorship.

We have solved Eq. (5.4) numerically using standard methods of integration for ordinary differential equations. We easily achieve high accuracy in spite of the fact that there is a regular singular point at x_1, where $\frac{1}{2}\bar{g}(x_1)=x_1$. By gradually reducing the integration step we approach x_1 and obtain an accurate estimate for $\theta(x_1)$ and x_1. We evaluate κ, using Eq. (5.4), from the calculated values of x_1 and $\theta(x_1)$ and compare it with the original κ to obtain an estimate of the numerical accuracy. For small κ values ($\kappa<0.4/\sqrt{4\pi}$) the difference between the two is less than 10^{-4} and it is less than 10^{-5} for the larger values ($\kappa>0.4/\sqrt{4\pi}$).

Differential values of κ yield different initial conditions on $[0,x_1]$, where $x_1=x_1(\kappa)$. $\theta(x_1)$ decreases with κ, while $2M/r|_{x_1}$ and x_1 increase with κ. The larger $2M/r|_{x_1}$, the more likely it is to form a black hole. On the other hand, as κ increases, $\theta(x)$ becomes less steep and the numerical errors decrease (see Fig. 9).

The solution of Eq. (5.4), which we call the interior solution, determines the spacetime only in the domain of dependence of the initial region $\{u=-1,0\leq r\leq x_1\}$. To obtain a global solution one has to specify initial data, $\theta(x)$, on $r>x_1$ and check whether a black hole forms before $u=0$ in the exterior region. With Christodoulou's construction it is impossible to specify vacuum as exterior initial data. Equations (5.4) and (5.3a) yield $h(x_1)\neq0$, and the choice $h=0$ for $r>x_1$ yields discontinuous initial data. One must supplement the solution of Eqs. (5.1), (5.3a), (5.3c) and (5.4) with nonvanishing causal exterior initial data at $r>x_1$, whose evolution might not be trivial. The global structure of the solution depends on the region exterior to the null geodesic, $r_1(u)$, that passes through $(u=-1,x_1)$. In particular, if a black hole forms at the exterior before $u=0$, the singularity at $(r=0,\ u=0)$ is not naked.

The inner solution provides inner boundary conditions for the exterior solution on $r_1(u)$. Using $r_{1,u}=x_1$ and the initial condition $r_1(u=-1)=x_1$, we obtain

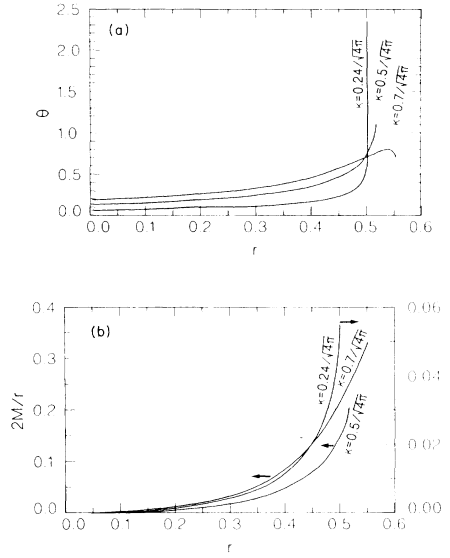

FIG. 9. Initial data at $u=-1$ and $0\le r\le x_1$. With $\kappa=0.24/\sqrt{4\pi}$, $\kappa=0.5/\sqrt{4\pi}$, and $\kappa=0.7/\sqrt{4\pi}$, (a) θ vs r and (b) $2M/r$ vs r.

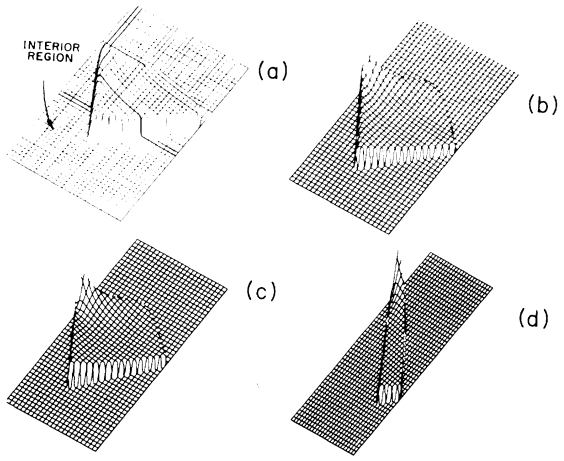

FIG. 10. $2M/r$ in the exterior region for (a) $\kappa=0.24\sqrt{4\pi}\,\theta(x>x_1)=\theta(x_1)2^{25}/(1+x/x_1)^{25}$, (b) $\kappa=0.5/\sqrt{4\pi}$ and $\theta(x>x_1)=\theta(x_1)2^{25}/(1+x/x_1)^{25}$, (c) $\kappa=0.7/\sqrt{4\pi}$ and $\theta(x>x_1)=\theta(x_1)2^{25}/(1+x/x_1)^{25}$, (d) $\kappa=0.5/\sqrt{4\pi}$ and $\theta(x>x_1)=\theta(x_1)(1-x)^{50}/(1-x_1)^{50}$.

$$h(u,r_1)=h(-1,x_1)-\kappa\ln(|u|)\,, \tag{5.5a}$$

$$\bar{h}(u,r_1)=\bar{h}(-1,x_1)-\kappa\ln(|u|)\,, \tag{5.5b}$$

$$g(u,r_1)=g(-1,x_1)\,, \tag{5.5c}$$

$$\bar{g}(u,r_1)=2x_1\,, \tag{5.5d}$$

$$\frac{2M(u,r_1)}{r_1}=\frac{2M(-1,x_1)}{x_1}\,. \tag{5.5e}$$

We choose external initial data and we calculate the exterior solution using the inner boundary conditions given by Eqs. (5.5a)–(5.5e). Figure 10 describes the evolution of $2M/r$ for different κ values and for two kinds of external continuation functions. We describe only the exterior region, i.e., the domain of dependence of the region $\{u=-1,\ x_1<r<r_{\max}\}$. We have found that (see also Fig. 11) a black hole always forms before $u=0$.

We now estimate from the initial data an upper limit, u_0 for $u_{\rm bh}$, at which a black hole forms. The amount of mass between any two shells remains constant as long as the shells have not arrived at the origin. In particular, the mass between r_n and x_1 remains constant until $u=0$:

$$M(-1,r_n(-1))-M(-1,x_1)=M(u,r_n(u))-M(u,r_1(u))\,. \tag{5.6}$$

Using the fact that $2M/r$ is constant along the null geodesic r_1 and that on r_1, $\bar{g}=2x_1$, we obtain

$$M(u,x_1)=-uM(-1,x_1) \tag{5.7}$$

and

$$M(u,r_n(u))=M(-1,r_n(-1))-(1+u)M(-1,x_1)\,. \tag{5.8}$$

Using Eq. (3.1b) and $\bar{g}_n(u)>\bar{g}_n(-1)$, we obtain

$$r_n(u)>r_n(-1)-\tfrac{1}{2}\bar{g}_n(-1)(1+u)\,. \tag{5.9}$$

A black hole forms when

$$\frac{2[M(-1,r_n)-(1+u)M(-1,x_1)]}{r_n}=1\,. \tag{5.10}$$

Therefore, a black hole forms before

$$u_0=\frac{\frac{1}{2}r_n(-1)-M(-1,r_n(-1))}{\frac{1}{4}\bar{g}_n(-1)+M(-1,x_1)}-1\,, \tag{5.11}$$

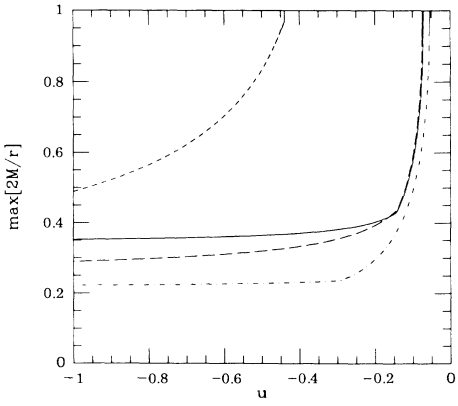

FIG. 11. $\max(2M/r)$ vs u for $\kappa=0.24/\sqrt{4\pi}$ and $\theta(x>x_1)=\theta(x_1)2^{25}(1+x/x_1)^{25}$ (short-dashed line); $\kappa=0.5/\sqrt{4\pi}$ and $\theta(x>x_1)=\theta(x_1)2^{25}/(1+x/x_1)^{25}$ (long-dashed line); $\kappa=0.7/\sqrt{4\pi}$ and $\theta(x>x_1)=\theta(x_1)2^{25}/(1+x/x_1)^{25}$ (solid line); and $\kappa=0.5/\sqrt{4\pi}$ and $\theta(x>x_1)=\theta(x_1)(1-x)^{50}/(1-x_1)^{50}$ (dashed-dotted line). A black hole always forms before $u=0$.

TABLE IV. Formation of a black hole in the exterior region of Christodoulou's initial data with the continuation functions $\theta(x>x_1)=\theta(x_1)2^{25}/(1+x/x_1)^{25}$ (first three lines) and $\theta(x>x_1)=\theta(x_1)(1-x)^{50}/(1-x_1)^{50}$ (last line).

κ	u_0	$u_{\rm bh}$	$2M/r$	r
$0.24/\sqrt{4\pi}$	−0.441 9	−0.470 24	0.999	0.267 6
$0.5/\sqrt{4\pi}$	−0.071 9	−0.074	0.997	0.086 4
$0.7/\sqrt{4\pi}$	−0.023 2	−0.083 9	0.999	0.103 8
$0.5/\sqrt{4\pi}$	−0.015	−0.054	0.997 6	0.054

i.e., $u_{\rm bh}\le u_0$.

For given initial data we calculate $u_0(r_n)$. If $u_0(r_n)<0$ for some r_n, then this initial data will evolve into black hole. Comparison of $u_{\rm bh}$ calculated from the complete evolution will u_0 calculated using Eq. (5.11) (see Table IV) demonstrates, as expected, that $u_0>u_{\rm bh}$ is always satisfied. The difference is large when the gravitational field is strong, e.g., for $\kappa=0.7/\sqrt{4\pi}$, since then $\bar{g}$ increase rapidly with u.

In a search for a naked singularity we have used Eq. (5.11) to estimate whether or not a black hole forms. We have chosen the following trial functions for the exterior initial data:

$$\theta(x)=\frac{\theta(x_1)\{1+\exp[(x_1-x_0)/a]\}}{1+\exp[(x-x_0)/a]}\ , \tag{5.12a}$$

$$\theta(x)=\frac{2^n\theta(x_1)}{(1+x/x_1)^n}\ , \tag{5.12b}$$

and

$$\theta(x)=\theta(x_1)\frac{(1-x)^n}{(1-x_1)^n}\ , \tag{5.12c}$$

where a and x_0 or n are free parameters. For each function we have looked for the maximal u_0 for several different choices of κ. The maximal u_0 was always obtained when the function decreased rapidly from $\theta(x_1)$ to zero. In other words, we have found that $u_0\to 0$ for $x_0\to x_1$ and $a\to 0$ or for $n\to\infty$. In none of the cases was $u_0\ge 0$. It seems that the discontinuous vacuum exterior is the only possible data that develops a naked singularity.

VI. CONCLUSIONS

We have studied the numerically spherical collapse of a massless scalar field. For a weak field, $2M/r$ is much smaller than unity and the scalar field converges inward, bounces, and disperses to infinity. When the initial field is stronger, $2M/r$ approaches unity and a black hole forms. In our coordinate system, g and $\bar{g}$ diverge and we cannot follow a black-hole appearance in this calculation. We can, still, estimate where and when a black-hole horizon appears from graphs of $2M/r$ or g. A black-hole appearance is also marked clearly on the trajectories of null geodesics, which converge inward in the (r,t) plane (see Fig. 1).

After testing the code and studying the evolution of Gaussian initial data we have considered the question of whether or not it is possible to obtain a naked singularity as a result of gravitational collapse of a massless scalar field. Christodoulou has suggested that special initial conditions at $u=-1$ exist which lead to a singularity at $u=0$, $r=0$. He was able to define uniquely the initial data only for $0\le r\le x_1$, for which he could solve the evolution equation analytically and show that a black hole does not form in the domain of dependence of $\{-1,0<r<x_1\}$. We have tried various extensions of the initial conditions that cover the region $x_1\le r\le\infty$. In all cases, a black hole formed before $u=0$. We believe that it is unlikely that one can construct a counterexample to cosmic censorship in this manner.

Recent results of Christodoulou[10] indicate that if a massless spherical scalar field forms a naked singularity, the scalar field must approach the form given by Eq. (5.1). Our results show, however, that such a singularity is most likely hidden inside a black hole. We conclude, therefore, that the spherical gravitational collapse of a massless scalar field cannot lead to a naked singularity.

ACKNOWLEDGMENTS

We would like to thank Dimitri Christodoulou for many valuable discussions. The research was supported in part by a National Science Foundation Grant No. PHY-8620266 to the Institute for Advanced Study.

[1]D. Christodoulou, in *Twelfth Texas Symposium on Relativistic Astrophysics,* proceedings, Jerusalem, 1984, edited by M. Livio and G. Shaviv [Ann. N.Y. Acad. Sci. **470**, 147 (1986)].
[2]D. Christodoulou, Commun. Math. Phys. **105**, 337 (1986).
[3]D. Christodoulou, Commun. Math. Phys. **106**, 587 (1986).
[4]D. Christodoulou, Commun. Math. Phys. (to be published).
[5]D. Christodoulou, Commun. Math. Phys. (to be published).
[6]R. Penrose, Riv. Nuovo Cimento **1**, 252 (1969).
[7]D. S. Goldwirth, MSc. thesis, Hebrew University, Jerusalem, 1986.
[8]M. Choptuik, Ph.D. thesis, University of British Columbia, 1986.
[9]D. Christodoulou (private communication).
[10]D. Christodoulou (private communication).
[11]J. M. Bardeen and T. Piran, Phys. Rep. **96**, 205 (1983).
[12]L. D. Lambert, *Computational Methods in Ordinary Differential Equations* (Wiley, New York, 1973).